lubricants

Review

The Preparation of Graphene Oxide and Its Derivatives and Their Application in Bio-Tribological Systems

Jianchang Li [1,2], Xiangqiong Zeng [1,*], Tianhui Ren [2] and Emile van der Heide [1,3]

[1] Laboratory for Surface Technology and Tribology, University of Twente, P.O. Box 217, 7500 AE Enschede, The Netherlands; E-Mails: lijianchang87@sjtu.edu.cn (J.L.); e.vanderheide@utwente.nl (E.H.)

[2] School of Chemistry and Chemical Engineering, Key Laboratory for Thin Film and Microfabrication of the Ministry of Education, Shanghai Jiao Tong University, Shanghai 200240, China; E-Mail: thren@sjtu.edu.cn

[3] Netherlands Organisation for Applied Scientific Research—TNO, P.O. Box 6235, NL-5600 HE Eindhoven, The Netherlands

* Author to whom correspondence should be addressed; E-Mail: x.zeng@utwente.nl; Tel.: +31-53-489-4390.

Abstract: Graphene oxide (GO) can be readily modified for particular applications due to the existence of abundant oxygen-containing functional groups. Graphene oxide-based materials (GOBMs), which are biocompatible and hydrophilic, have wide potential applications in biomedical engineering and biotechnology. In this review, the preparation and characterization of GO and its derivatives are discussed at first. Subsequently, the biocompatibility and tribological behavior of GOBMs are reviewed. Finally, the applications of GOBMs as lubricants in bio-tribological systems are discussed in detail.

Keywords: graphene oxide; graphene oxide-based materials; biocompatibility; bio-tribology

1. Introduction

The study of graphene has been one of the most exciting topics in material science and many other research fields since the first report of the preparation and isolation of single graphene layers in 2004 [1]. Graphene, which consists of a single atomic layer of sp^2 two-dimensional (2D) hybridized

carbon atoms arranged in a honeycomb structure, is a basic building block for all graphitic forms [2]. 0D fullerenes, 1D nanotubes and 3D graphite are all derived from 2D graphene. There is intensive attention on various applications of graphene, because of its unusual properties, such as high Young's modulus values, excellent thermal conductivity and the mobility of charge carriers [3]. The initial application of graphene was in the field of electronic devices, concentrated upon its electronic properties [4–6]. As the research on graphene developed rapidly, it was soon realized that graphene possesses other exciting properties, such as high stiffness and strength, excellent thermal properties and promising biocompatibility [7]. As early as 2007, Geim [2] predicted a wide range of applications for graphene and graphene-based materials.

However, there are two main problems. One is how to produce graphene sheets at a sufficient scale. As we know, graphite, despite that it is inexpensive and available in large quantities, does not readily exfoliate to yield monolayer graphene sheets. The other is that graphene sheets are hard to be incorporated and distributed homogeneously into various matrices for applications. Graphite oxide, containing abundant oxygen-based groups, not only can be obtained easily from the oxidation of graphite, but can also be readily exfoliated to graphene oxide (GO) nanosheets using ultrasonic devices. In fact, GO has been studied for a much longer period time than graphene. GO is viewed as the precursor to produce graphene (reduced GO) by chemical and thermal reduction. Furthermore, in recent years, many GO derivatives, such as GO-based composites, GO-based coating and thin films, as well as GO-based nanoparticles, emerged as functional materials for various applications.

This review focuses on GO and GO-based materials (GOBMs), as well as their biocompatibility and tribological performance. The preparation and characterization of GO are presented at first. Subsequently the preparation and characteristics of its derivatives are discussed. After that, the biocompatibility and specific tribological behavior are reviewed. Finally, the possibilities to use GOBMs for bio-tribological applications, such as artificial joint replacement, is discussed in detail.
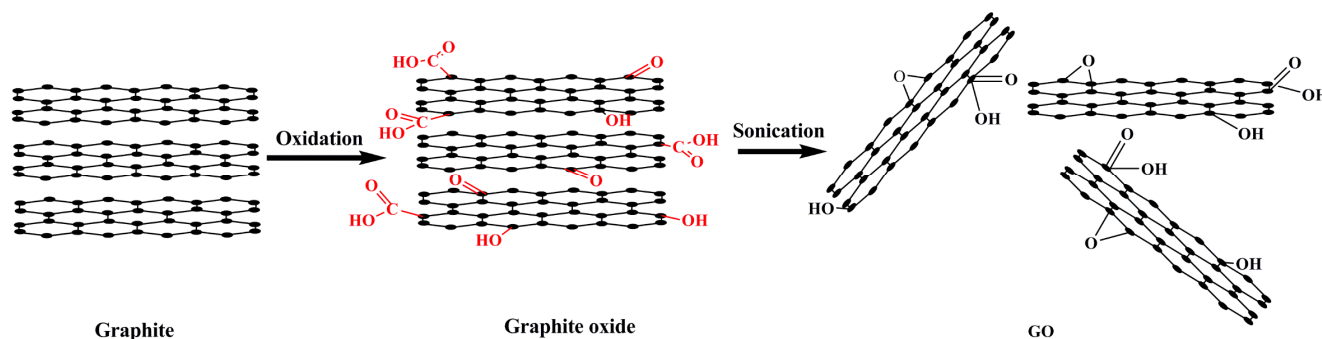
2. Preparation of GO

Although the strong σ_{C-C} bond and π bond give graphene exceptional physical properties, it also contributes to the weak reactivity of graphene, which, in turn, limits its use in engineering applications. GO has an abundance of oxygenated functional groups, providing possible use in various applications, after chemical modification.

Graphite, the raw material for preparing GO, consists of polycrystalline particles or granules and can be selected from natural and synthetic sources. Natural graphite is the most common source and is used in a wide range of applications that use chemical modifications [8]. It is because natural graphite contains numerous localized defects in its π-structure that these may serve as seeding points for chemical reaction processes [3].

The route to prepare GO involves two main steps; see Figure 1. Firstly, graphite powder is oxidized to produce graphite oxide, which can be readily dispersed in water or another polar solvent due to the presence of hydroxyl and epoxide groups across the basal planes of graphite oxide and carbonyl and carboxyl groups located at the edges [9–11]. Secondly, the bulk graphite oxide can be exfoliated by sonication to form colloidal suspensions of monolayer, bilayer or few-layer GO sheets in different

solvents [3]. The critical point of preparing GO is the selection of suitable oxidizing agents to oxidize graphite.

Figure 1. Preparing graphene oxide (GO).

Reviewing the origin of the preparation of graphite oxide, it has had more than 150 years of history since the first report from Brodie [12] in 1859. The oxidation process was performed by adding $KClO_3$ in a single addition to a slurry of graphite in fuming HNO_3. The C/H/O ratio of the oxidation product was determined to be 2.19/1.00/0.80, which is the typical composition of graphite oxide [13]. About 40 years later, Staudenmaier [14] modified the Brodie method by using concentrated H_2SO_4 and fuming HNO_3 as the oxidizing agents. Additionally, the $KClO_3$ was added slowly and carefully over a period of one week in the procedure. In the following decades, many other similar methods have been reported [15,16]. The method most commonly used today was reported by Hummers in 1958 [17]. In the Hummers method, the oxidation of graphite to graphite oxide is accomplished by treating graphite with essentially a water-free mixture of concentrated H_2SO_4, $NaNO_3$ and $KMnO_4$. Compared to the Brodie-Staudenmaier methods, the Hummers method requires less than 2 h for completion at temperatures below 45° and can be carried out safely. These three methods are the primary routes to prepare graphite oxide from graphite and have been reviewed extensively by Ruoff and co-workers [18,19].

However, all three reactions involve the liberation of toxic gas NO_x and/or ClO_2. Some modifications based on the Hummers method have been proposed. Kovtyukhova [20] added a pre-oxidized procedure using H_2SO_4, $K_2S_2O_8$, and P_2O_5. The C/O ratio of the oxidation product was 4.0/3.1, illustrating that this was richer in oxygen than the graphite oxide prepared by the Hummers method. The method proposed by Kovtyukhova is defined as a typical modified Hummers method and has been cited by many researchers in recent years [21–23]. In 2010, Marcano [24] found another method, which is named the "improved Hummers method" here, in this work (Figure 2). By adding H_3PO_4 to the formation of graphene oxide nanoribbons (GONRs) from multiwalled carbon nanotubes, it shows that more GONRs were produced with more intact graphitic basal planes [25]. The improved Hummers method, using $KMnO_4$, H_2SO_4, and H_3PO_4 as the oxidizing agents, avoids the release of NO_x and yields a greater amount of hydrophilic oxidized graphite material compared to the original Hummers method. Due to its simpler protocol and equivalent conductivity upon reduction, the improved Hummers method is attractive for preparing GO on a large scale. Recently, Li [26] reported that GO prepared by the improved Hummers method could obtain a high grafting rate of poly (L-lactic acid) (30.8%) at a moderate condition.

Figure 2. Preparation procedures of GO (adapted from [23]).
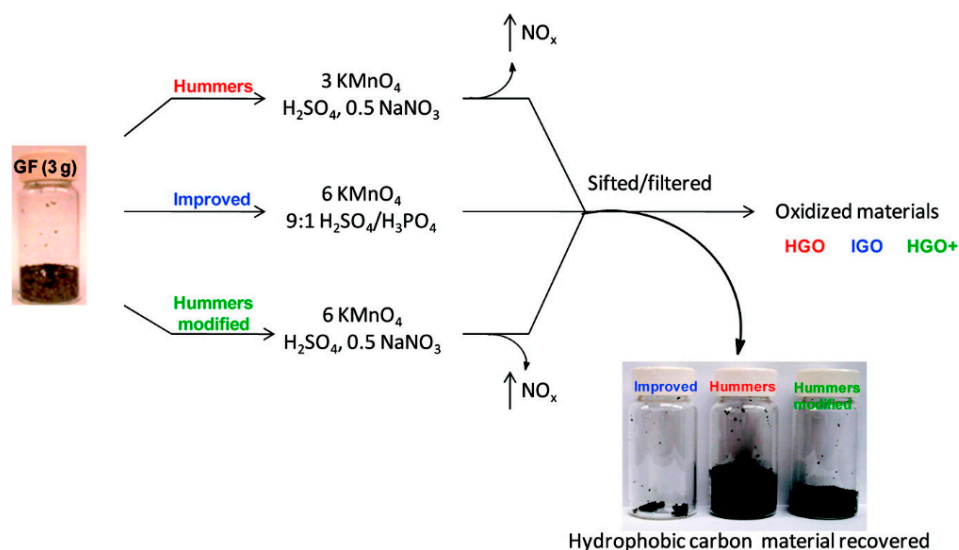
3. Characterization of GO

The structures and topographies of graphite oxide and GO can be analyzed in detail by a number of techniques.

Solid-state ^{13}C nuclear magnetic resonance (NMR) is a significantly effective means to explore the chemical structures of GO [27]. The most well-accepted structure model of GO (Figure 3) was proposed by Lerf [10,11] using this technique. It suggests that the structure of GO involves aromatic regions with unoxidized benzene rings and regions with aliphatic six-membered rings containing hydroxyl, epoxide, carbonyl and carboxyl groups.

Figure 3. Structure model of GO (adapted from [11]).
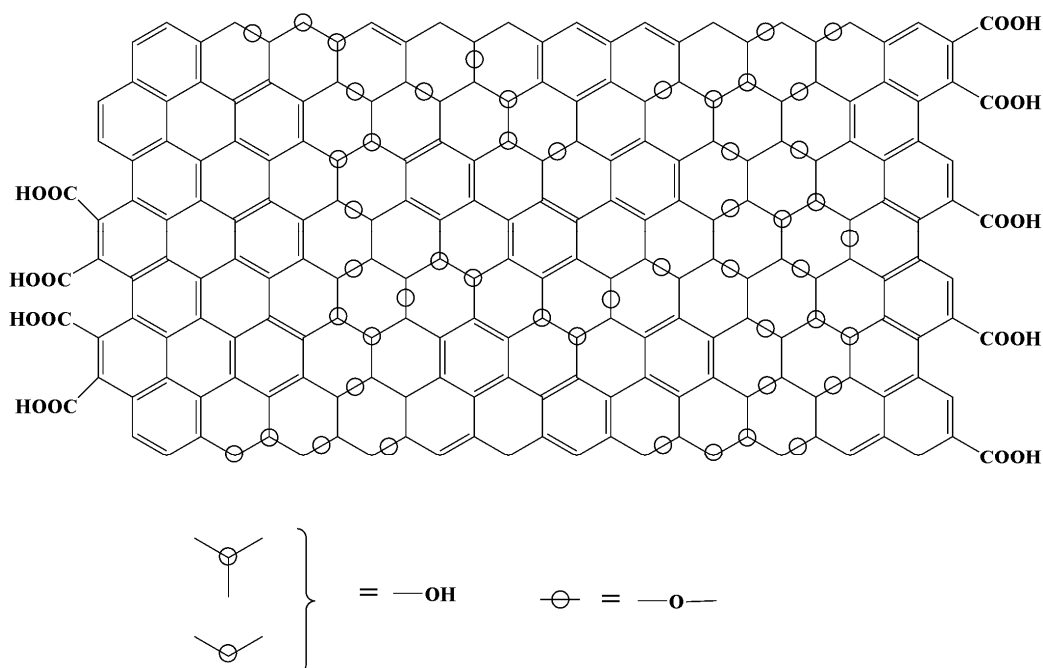
Using X-ray diffraction (XRD), the degree of oxidation of graphite and the interlayer spacing can be obtained. With graphite being oxidized to graphite oxide, the sharp reflection of graphite at $2\theta = 25 \sim 30°$ disappears, and a new peak at $2\theta = 10 \sim 15°$ that corresponds to graphite oxide appears [28]. McAllister [29] reported XRD patterns of graphite oxide prepared by the Staudenmaier method for various lengths of oxidized time, suggesting that the reaction process can be monitored by using XRD. The absence of a peak at $2\theta = 25 \sim 30°$ indicates that graphite is converted into graphite oxide completely. The interlayer spacing *d* of graphite and graphite oxide can be calculated according to the Bragg law:

$$n\lambda = 2d\sin\theta \qquad (1)$$

where *n* is the diffraction series and λ is the X-ray wavelength. The native sharp peak of graphite is at $2\theta \sim 26°$, and the graphene layer spacing *d* is about 0.34 nm. In general, the GO interlayer spacing *d* in graphite oxide is around 0.6–1.0 nm depending on the degree of oxidation of graphite and the amount of water molecules intercalated into the interlayer spacing [28].

Multi-mode atomic force microscopy (AFM) is the foremost method to quantify the thickness of GO sheets. The thickness of GO sheets is approximately 1 nm by AFM measurement, which illustrates that graphite oxide is successfully exfoliated to GO nanosheets [19,30,31].

The chemical analysis of GO can be conducted using X-ray photoelectron spectroscopy (XPS) and Fourier transform infrared (FTIR). The XPS spectrum of C 1s is divided into four peaks, which represent different kinds of functional groups (Table 1). The epoxide group (C–O–C) of graphite oxide has a C 1s binding energy similar to C–OH [30].

Table 1. The binding energy (eV) of C 1s in various functional groups from the XPS spectrum.

Item	C–C	C–O (Hydroxyl and Epoxy)	C=O	O=C–OH	Reference
	284.8	286.3	287.2	288.4	[30]
	284.6	285.8	287.1	288.9	[31]
Bonding Energy (eV)	285.1	286.4	287.8	288.9	[32]
	284.8	286.2	287.8	289.0	[33]

Due to strong resonance Raman scattering in graphene-based materials [34–37], Raman spectroscopy has been extensively employed to characterize GOBMs in recent years [38]. A distinct difference between the Raman spectrum of GO and graphene can be seen from Figure 4. Graphene shows a single sharp peak G band at $\sim$1580 cm^{-1}, which corresponds to the vibration of sp^2 carbon. For GO, the G-band blue-shifts to $\sim$1590 cm^{-1} and becomes broader compared to graphene, and a new broad, intense peak D-band appears at $\sim$1330 cm^{-1}, which corresponds to sp^3 carbon and defects associated with vacancies and grain boundaries [38–40]. Therefore, the intensity ratio of the D- and G-band is related to the microstructure of GO.

Figure 4. Raman spectra of monolayer GO and monolayer graphene (adapted from [39]).
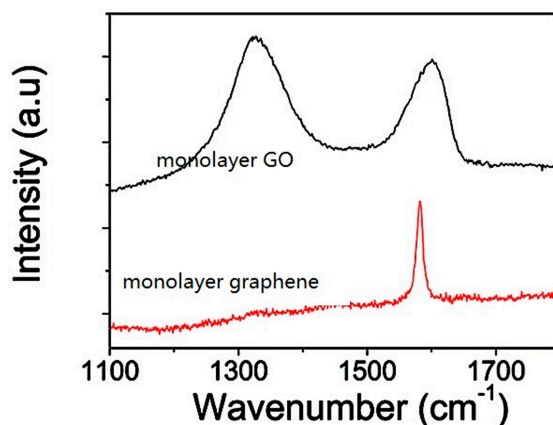
High-resolution transmission electron microscopy (HR-TEM) is also used to study the microstructure of GO [37,41–43]. It is found that there are three major features in GO: holes, graphitic regions (graphene-like) and high contrast disordered regions, which indicate areas of high oxidation [41]. The formation of holes in GO is due to the release of CO and CO_2 during the processes of oxidation and sheet exfoliation [44]. Pacile [42] also confirmed that the structure of GO sheets consists of ordered regions along with disordered oxygen-containing functional group areas.

## 4. Derivative of GO and Their Characteristics

GOBMs can be prepared from a GO precursor and employed for a wide range of application. The GOBMs discussed in this section include: (1) the reduced-GO (RGO); (2) the functionalized GO; (3) GO-based thin films; and (4) GO-based nanocomposites.

4.1. RGO

One of the aims to prepare GO is to produce graphene-like carbon materials at a large scale by a reduction process [45–48]. GO reduction is a process that converts sp^3 carbon to sp^2 carbon. The reduced product is referred to as graphene-like, rather than graphene, because in most cases, it is impossible to reduce GO fully back to graphene [43,48]. Therefore, RGO is defined as the reduction derivative of GO, although the electrical, thermal, mechanical properties and surface morphology of RGO and pristine graphene are similar.

RGO can be obtained from GO through various reduction methods. One of the mostly used chemical reduction methods was reported by Stankovich [34] utilizing hydrazine hydrate ($N_2H_4 \cdot H_2O$) as the reductant. The simplified pathway and proposed reduction mechanism are described in Figure 5. Other reductants, such as dimethyl-hydrazine [45], hydroquinone [49] and $NaBH_4$ [48,50,51], have also been employed to prepare RGO. However, using chemical reduction methods may introduce heteroatom nitrogen that affects the electronic structure of RGO. Another commonly used method is thermal reduction by heating GO to above 1000 °C [22,52,53]. Besides, some other novel reduction methods, such as the photo-catalytic method [54–56], biomolecule-assisted methods [57,58], plant extract method [59], supercritical fluid method [60] and electrochemical method [61], were proposed for the reduction of GO.

Figure 5. (**a**) The idealized and simplified pathway and (**b**) the proposed reduced mechanism for the reduction of GO by hydrazine hydrate (**a,b** adapted from [34,62], respectively).
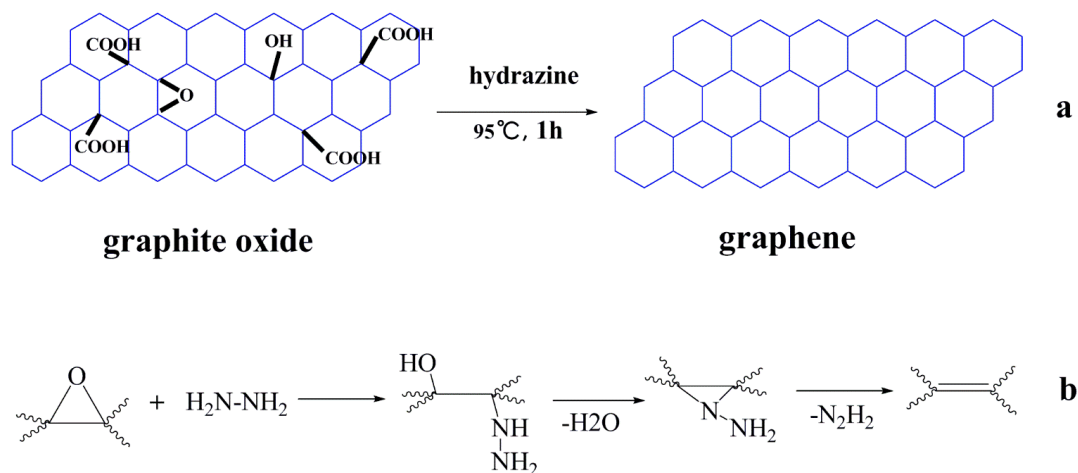
The C 1s XPS spectrum of RGO is quite different from that of GO, as Figure 6 shows; the peak intensities of oxygen-containing groups are much weaker than that of GO, indicating that most of the oxygen-containing groups have been removed from GO successfully, through reduction treatments. Raman spectroscopy shows that the I(D)/I(G) ratio decreases from 1.3 ± 0.3 to 0.8 ± 0.2, which is also indicative of the decrease in the fraction of non-graphitic carbon in the monolayers [63].

Figure 6. The C 1s XPS spectra of: (**a**) GO; (**b**) RGO (adapted from [34]).
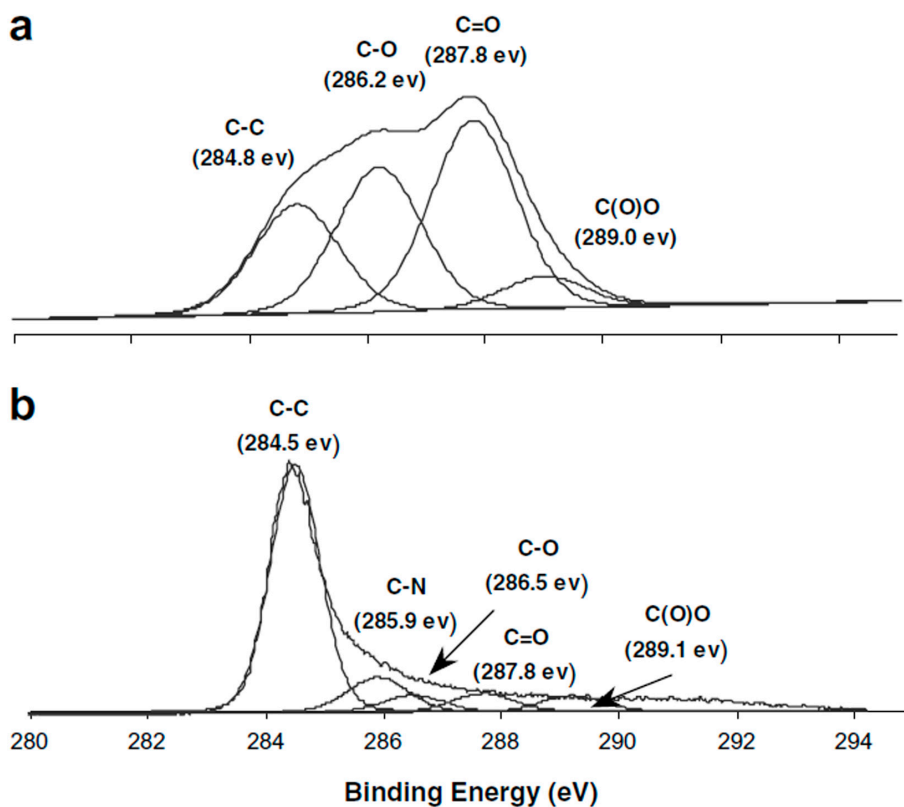
4.2. Functionalized Derivatives of GO

Functionalization of GO comprises chemical reactions involving covalent and non-covalent modifications in order to add other functional species to GO platelets to form GO derivatives. From the structure model of GO, given in Figure 4, it is clear that GO has numerous reactive groups, making it possible to be covalently functionalized with a great number of modifying reagents. Non-covalent interactions of GO primarily involve van der Waals interaction and π–π stacking. Table 2 lists the covalent and non-covalent modifications of GO by reacting with different functional groups on GO. Functionalized GO derivatives can fulfill specific requirements for various applications.

Table 2. The covalent and non-covalent modifications of GO using different modifying agents.

Reactive Groups	Modifiers	References
Epoxy	Aliphatic amines	[64–68]
	Aromatic amines	[69,70]
	Dopamine	[71]
	Amino acid	[64]
	Ionic liquid (amine-terminal)	[72]
Carboxylic acid	ethylenediamine, 1,6-hexanediamine	[73]
	Amine-functionalized porphyrin Pyrrolidine fullerene	[74]
	N-Containing heterocyclic compounds	[75]
Hydroxyl	Polyoxyethylene sorbitol anhydride monolaurate	[76]
π–π stacking	Polyaniline	[77]

The epoxy groups of GO can be easily attacked by nucleophilic regents, resulting in a nucleophilic substitution reaction to open the epoxy rings. The typically used nucleophilic reagents are organic amine compounds bearing a lone pair of electrons. Wang [68] employed octadecylamine for the modification of GO, followed by reduction by hydroquinone to prepare organophilic graphene that is soluble in various organic solvents. In a later study [70], p-phenylenediamine (PPD) is attached to GO through the reaction with epoxy groups generating GO-PPD. Then, GO-PPD is modified with cyanuric chloride (CC) and grafted with maleic anhydride-grafted polypropylene (MAPP) to fabricate functionalized GO/PP (fGO/PP) nanocomposites. The structure of fGO/PP nanocomposites can be seen in Table 2. The introduction of fGO to PP nanocomposites significantly improves the thermal stability, thermal conductivity and mechanical properties of PP nanocomposites. Ionic liquid with an amine end group is also used to functionalize GO [72], the resulting GO's derivatives can be well-dispersed in polar medias (water, dimethylformamide, dimethyl sulfoxide).

Numerous GOBMs can be derived based on the reaction with carboxylic acid groups on GO sheets. Acylation and esterification reactions are frequently used approaches to modify GO. After the activation of carboxylic acid groups by 2-(7-aza-1*H*-benzotriazole-1-yl)-1,1,3,3-tetramethy-luroniumhexa-fluorophosphate (HATU), Yan [73] employed two different diamines, ethylenediamine (EA) and 1,6-hexanediamine (HA) to react with GO, producing diamine-functionalized GO (AGO),

and found that AGOs display higher thermal stability than GO, and the EAGO shows excellent dispersibility in DMF compared to GO. Amine-functionalized porphyrin (TPP-NH$_2$) and pyrrolidine fullerene, respectively, are also used for the functionalization of GO by a mild coupling reaction between the –NH$_2$ group of TPP-NH$_2$ (or the –OH group of pyrrolidine fullerene) and the –COOH group of GO [74]. It is noticed that carboxyl groups are first activated by thionyl chloride SOCl$_2$. Aside from HATU and SOCl$_2$, other coupling agents, such as 1-ethyl-3-(3-dimethylaminopropyl)-carbodiimide (EDC) [78] and *N'*,*N'*-dicyclohexylcarbodiimide (DCC) [79], are also used for the activation of carboxylic acid groups. Recently, N-containing heterocyclic compounds-functionalized GO (see Table 2) was demonstrated to improve the thermal stability of GO and to have good solubility in organic solvents, suggesting the potential of using it as an additive for polymeric systems [77].

The non-covalent approach is very promising, as it preserves the native physical properties of GOBMs to the maximum extent without sacrificing the sp^2-conjugated structure. In recent years, many research papers concerning non-covalent functionalization of GO have been published and have provide great value to the study of graphene and GO-based materials for different applications [78–84].

Lu [78] reported the synthesis of Au nanoparticles (AuPNs) on polyoxyethylene sorbitol anhydride monolaurate (TWEEN 20)-functionalized GO (AuPNs/TWEEN/GO) by non-covalent interactions between TWEEN 20 and GO, in which TWEEN 20 was used as a stabilizing agent for GO. The three-terminal hydroxyl groups in TWEEN 20 are hydrophilic and can from hydrogen bond with the –OH groups of GO. The aliphatic chain in TWEEN 20 can easily be adsorbed on the hydrophobic part of GO by van der Waals force. After fabricating the TWEEN/GO, the AuPNs was grafted onto the surface of TWEEN/GO by *in situ* chemical reduction of gold salts. The AuPNs/TWEEN/GO composites exhibit a remarkable catalytic performance for hydrazine oxidation and good activity in catalyzing the reduction of 4-nitrophenol (4-NP) by NaBH$_4$, indicating that such AuPNs/TWEEN/GO composites may be very promising for applications in biosensing, environmental monitoring, analytical chemistry and electro-analytical chemistry [78].

A novel kind of GOBM, Fe$_3$O$_4$-SiO$_2$-polyaniline–GO composite (MPANI-GO), was prepared by a simple non-covalent interaction of π–π stacking of GO with Fe$_3$O$_4$-SiO$_2$-polyaniline [79]. The oxygen-containing functional groups of GO can bind with metal ions, especially the multivalent metal ions, which makes GO an ideal adsorbent for metal ions. GO is hard to fully recover from aqueous solution because of its high hydrophilicity and good dispersibility [85]. Therefore, Fe$_3$O$_4$-SiO$_2$ nanoparticles are introduced at the surface of GO. After this, the MPANI-GO composite is applied successfully to magnetic solid phase extraction (MSPE) of traces of rare earth elements in tea leaves and environmental water samples [79].

4.3. GO-Based Thin Films

GO-based thin films are another kind of important GOBMs. GO sheets can be deposited on virtually any substrate in the form of thin films using different techniques [86]. Table 3 briefly summarizes the techniques and (potential) applications of various GO-based thin films on different substrates.

Table 3. Various GO-based thin films and their applications.

Substrates	Techniques	Applications or Potential Applications	References
Ti	Electrophoretic deposition (EPD)	Corrosion protection Biomedical	[87,88]
TiO₂	Spin-coating	Photocatalytic	[89]
	Solvothermal		[90]
	Aqueous deposition		[91]
SiO₂	Sol-gel approach	Environment	[92]
	Spin coating	Humidity sensors	[93]
Si	Spin-coating	Transparent conductors	[94]
	Langmuir-Blodgett/dip-coating	Transparent conducting thin films	[95]
	Grafting-onto	Lubricants	[96]
	Covalent assembly	Lubricants	[32]
	EPD	Lubricants	[97]
PMMA	Covalent immobilization	Microfluidic bioreactors	[98]
Cu	EPD	Corrosion resistance	[99,100]
	Electrochemical deposition	Corrosion resistance	[101]
Cordierite	Hydrogen bonding	Catalysts	[102]
Al foil	Spin-coating	Hybrid transparent conductive films	[103]

Li [87] prepared ternary graphene oxide-hyaluronic acid-hydroxyapatite (GO-HY-HA) coatings on a titanium substrate (GO-HY-HA/Ti) using the electrophoretic deposition (EPD) method employing hyaluronic acid as a charging additive and dispersion agent; see Figure 7. The GO-HY-HA/Ti thin films show enhanced corrosion protection of the Ti substrate and, as such, are possibly suited for applications in the biomedical field. This is confirmed by Li [88], giving evidence for the biocompatibility of GO-based HA.

GO-based thin films are used in certain electronic applications. Watcharotone [94] reported the first example of a transparent and electrically-conductive ceramic composite of GO-based films on glass and hydrophilic SiO$_x$/silicon substrates using a spin-coating technology. Domingues [103] prepared a reduction of graphene oxide films on Al foil using spin-coating technology. It is found that such films have good electrical conductivity and optical properties and can be used as hybrid transparent conductive films.

Figure 7. Illustration of the experimental setup (**a**) and mechanism (**b**) of the electrophoretic deposition (EPD) process for preparing GO-hyaluronic acid-hydroxyapatite (GO-HY-HA) nanocomposite coatings (**c**) on Ti substrate (adapted from [87]).
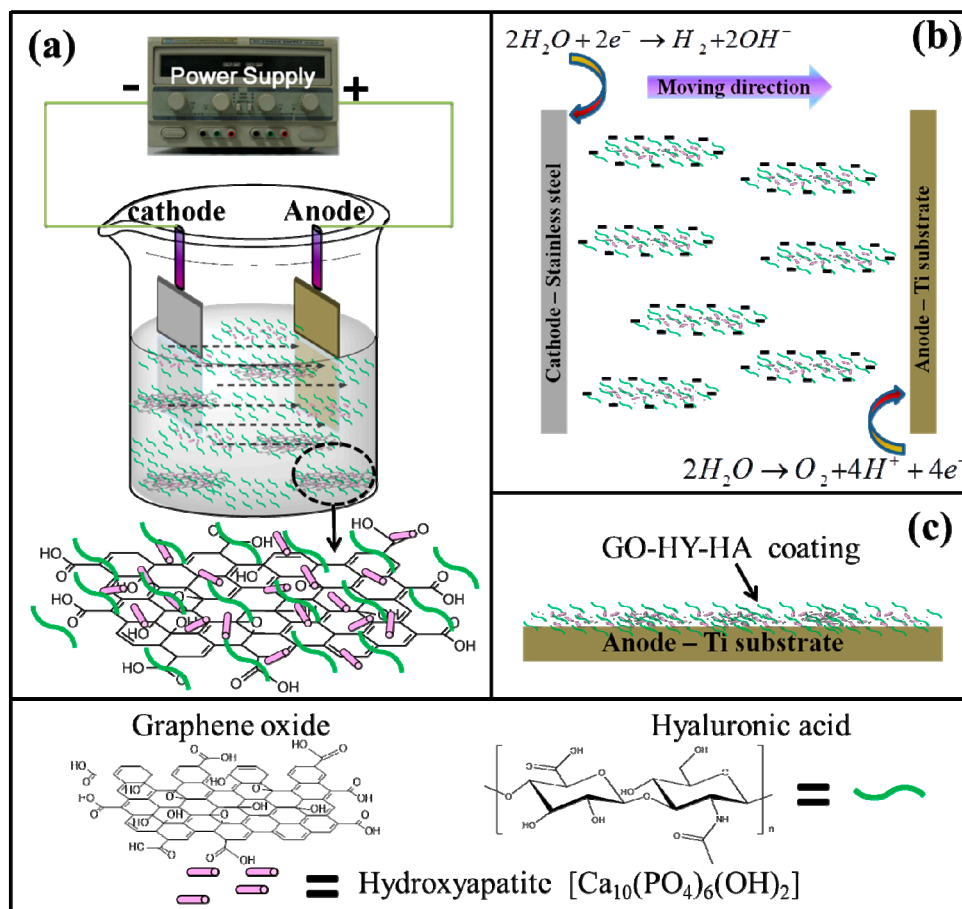
4.4. GO-Based Nanocomposites

Graphene-based additives or fillers are thought to improve specific properties of materials; see especially the paper of Geim [2]. The addition of such fillers could, e.g., lead to a significant improvement in the mechanical properties, electrical conductivity and thermal conductivity of polymer-based materials. However, graphene not only has poor dispersibility in either aqueous or nonaqueous solvents, but also is chemically inert, preventing any kind of interaction with the polymer matrices. GO-based additives or fillers are more suited for the manufacturing of polymer-based composite materials, as can be readily obtained in large quantities, and exfoliate and disperse in a polymer matrix. The most obvious reason for GO as a promising filler for polymer is that its oxygen-containing functional groups can bond with a polymer matrix to form a strong interface. One of the challenges remains the distribution of the fillers [104]. Ultrasonication dispersion [105], hot-pressing [106] and ball milling [107] techniques are used to distribute GO for preparing GO/UHMWPE nanocomposites. *In situ* polymerization is the most common and highly efficient method for preparing GO-based composites. Polyethylene- [108], polypropylene- [109], poly(methyl methacrylate)- [110], polypyrrole- [111,112], polyaniline- [113], polyurea- [114] and copolymer- [115] matrix GO nanocomposites are successfully prepared by using *in situ* polymerization.

Evidence for the improvement of properties is, for example, given for GO/PMMA (poly(methyl methacrylate)) nanocomposites, which show a large shift of over 15 °C in the glass transition temperature (T_g) and show a higher elastic modulus, as much as 128% *versus* neat PMMA [110]. The fracture strength of GO/PMMA nanocomposites is much higher than that of pure PMMA. Amin-functionalized GO can reinforce the thermal stability, storage modulus and tensile strength of the pure polyurea [114]. The electrical conductivity of sulfonated, reduced GO/PPy (polypyrrole) nanocomposites is 50 S·cm^{-1}, while the electrical conductivity of pure PPy is 0.65 S·cm^{-1} [112]. The performances of super-capacitor cells based on the sulfonated, reduced GO/PPy nanocomposites were evaluated, and the results show that the composites exhibited not only excellent high-rate discharge ability, but also a desirable cycle life. The sulfonated, reduced GO/PPy nanocomposites are promising electrode materials for supercapacitors.

5. Biological Property of GO-Based Materials

One of the preconditions of GOBMs applied in bio-tribological systems is that they would be biocompatible. It is well known that the biocompatibilities of materials depend on their intrinsic structures and properties, as well as the production methods used [7].

Ruiz [116] studied the antibacterial, bacteriostatic and cytotoxic properties of GO in both bacteria and mammalian cells. The results show that bacteria in 25 μg/mL colloidal GO Luria-Bertani (LB) media grow faster than in LB media without colloidal GO, indicating that GO may be acting as a scaffold for bacterial attachment, proliferation and biofilm formation. Bacterial growth on a surface coated with GO is two- and three-times better than on a surface without GO. Similarly, GO is shown to greatly enhance the attachment and proliferation of mammalian cells. Liu [117] considered that the existence of the hydrophilic groups contributes to be good biocompatibility of GO sheets.

Some references revealed that hydrophilic GO is able to penetrate cell membranes, resulting in cytoplasmatic, perinuclear and nuclear accumulation [118–120]; while this behavior of GO can be inhibited by chemical or physical functionalization with polymers [120]. Furthermore, GO increases the surface hydrophilicity of the biocomposites, leading to improved biocompatibility [121]. Furthermore, the introduction of GO to polymers may generate a favorable surface topography toward cell adhesion [122]. Chen [105] studied the biocompatibility of GO/UHMWPE composites. Figure 8 shows that the cells are well adhered and proliferated on the GO/UHMWPE scaffold with the increase of the culture time till the sample surface is almost totally covered with cells after 90 h of incubation, indicating the excellent biocompatibility of GO/UHMWPE composites. This is attributed to the good intrinsic biocompatibility and the hydrophilic nature of GO. Yan [123] obtained a similar conclusion when studying the biocompatibility of GO-polyaniline and graphene-polyaniline hybrid papers. Gurunathan [124] observed that microbially-reduced graphene oxide (M-rGO) exhibits significant biocompatibility for primary mouse embryonic fibroblast (PMEF) cells. Many researchers investigate the cytotoxicity properties of GO. Some of them conclude that GO materials are limited or not cytotoxic to human cells [125–127]. However, Liao [128] reports that GO materials are cytotoxic to human erythrocytes and skin fibroblasts. Recently, Liu [129] adapted three cell lines (HUVEC, RAW264.7 and L929) to study the cytotoxicity of GO and phosphorylcholine oligomer-grafted GO (GO-PCn). The GO sheets cause damage to the HUVECs and RAW264.7, while GO-PCn presents no

cytotoxicity to them. However, L929 show a greater resistance to GO. On the one hand, GO has a huge specific surface area and a hydrophobic conjugated aromatic structure that can attract and adsorb the cell membrane component biomolecules, such as peptide, protein and other molecules with a hydrophobic moiety, resulting of wrapping the cells, affecting the normal function of the cell membrane [129]. On the other hand, after grafting the phosphorylcholine moieties, the surface of GO-PCn was likely covered by hydrophilic phosphorylcholine oligomer, which hindered the interaction of the conjugated aromatic structure with the cell membrane component molecules, thus improving the biocompatibility of GO [129]. This study indicated that even if GO is cytotoxic, GO-based materials would not be cytotoxic, suggesting that GOBMs would be applied in bio-systems in the future.

Figure 8. Fluorescent microscopy images of MC3T3-E1 cells on the GO/UHMWPE composite with 0.5 wt% GO for 24 h (**a**), 48 h (**b**) and 96 h (**c**) (adapted from [105]).
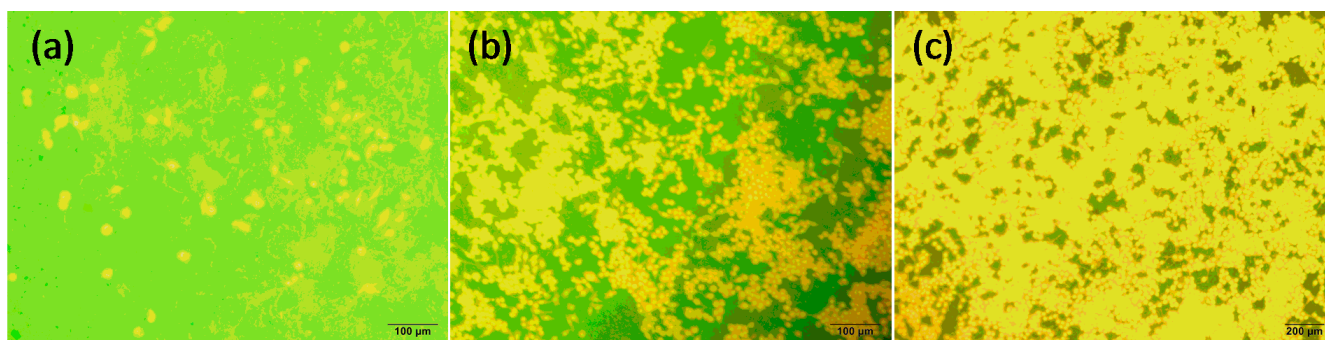
6. Tribological Behavior of GOBMs

GOBMs are expected to have good tribological performances in appropriate systems, because they are regarded as derivatives of self-lubricating graphite, which has a layered structure and exhibits a low friction and wear rate when used as solid lubricants. GOBMs have good mechanical properties, such as high a Young's modulus and hardness [45], making it feasible for them to be employed in tribological applications. Moreover, multiform GOBMs can be obtained readily through physical and chemical approaches due to abundant oxygen-containing groups in the GO sheets. Therefore, GOBMs could be promising materials used as solid lubricants, as fillers to reinforce the wear resistance of polymers and as water-based or oil-based lubricant additives. In all, GOBMs are promising lubricant materials with wide ranging applications in micro-/nano-electromechanical systems (MEMS/NEMS), functional additives, composites and bearing materials.

Ou [32,130] investigated the micro-/nano-tribological behaviors of 3-aminopropyl triethoxy-silane (APTES)-modified GO and RGO sheets (APTES-GO, APTES-RGO) on silicon substrate as solid lubricants. Results show that GO and RGO exhibit friction-reducing and antiwear properties at low applied loads. Valentini [96] confirmed this. Li [131] observed that a RGO nano-layer absorbed on a titanium alloy substrate presents a friction-reducing property and wear resistance. Liang [97] reported that using GO film as solid lubricants, the friction coefficient of a silicon wafer in sliding contact with steel balls is reduced to 1/6 of its value, and the wear volume is reduced to its 1/24, due to the GO films being soft compared to the silicon wafer. What is more, the friction coefficient of the film on the

Si wafer seems to be correlated to the roughness of the film, so the rougher film generates higher friction [97]. Because of the micro-/nano-thickness, GO- or RGO-based films are suited as solid lubricants for MEMS/NEMS.

GO and its derivatives are regarded as efficient nanofillers for polymers to improve their tribological properties. GO can significantly lower the wear rate and increase the friction coefficient of epoxy composites, which are widely used as antiwear materials in brake applications, where constant and high friction is needed [132,133]. This is due to the wrinkled surface morphology of GO, which would roughen the surface of the composite. GO/nitrile composites show better friction-reducing and antiwear properties than pure nitrile polymers [134,135]. Thangavel [136] demonstrated that poly(vinylidene fluoride)-functionalized graphene oxide (PVDF-FGO) nanocomposite thin films show a high resistance to wear and can be potentially used in microelectronic devices. RGO platelets serve as excellent wear reducers when incorporated as fillers in a PTFE matrix [137].

GOMBs show excellent tribological properties when used as lubricant additives in oil and aqueous media. Oleic acid-modified RGO is able to improve the friction-reducing and antiwear properties of gear oil (polyalphaolefin-9) at a low concentration [138]. GO-based engine oil nanofluids exhibit improved tribological properties [139]. Alkylated GO in organic solvents significantly improves the lubricity by reducing the friction coefficient and wear scar diameter (WSD) [140]. Song [141] studied the tribological behavior of GO in pure water for the first time and found that the water with GO nanosheets shows better tribological properties than the pure water and the water with oxide multiwall carbon nanotubes (CNTs-COOH). Recently, Kinoshita [142] also reported that adding GO particles into water improves lubrication and provides a very low friction coefficient with virtually no wear. The applications of GO sheets as a water lubricating additive create favorable conditions for the bio-tribological application of GOBMs.

7. Application of GOBMs in Bio-Tribological Systems

From the discussions in Sections 5 and 6, it was concluded that GO and its derivatives have excellent biocompatibility and promising tribological performance in an aqueous medium. GO derivatives are expected to be novel materials suited for demanding biomedical environments. In fact, GOBMs have already been investigated in artificial joint implants, although the literature about these parts is small [31,88,105,106,143–145].

UHMWPE has been used as a bearing surface in total joint replacements (TJRs) since 1962 [146] because of its unique characteristics, such as good biocompatibility, high wear resistance and low friction coefficient [143]. However, pure UHMWPE polymer still cannot fulfill the medical grade requirements, due to its low Young's modulus and low load bearing. Therefore, many types of fillers are under research to improve the tribological behavior of UHMWPE. Tai [106] reported that GO sheets added into UHMWPE can improve its tribological performance. The GO/UHMWPE nanocomposites are fabricated by hot-pressing with different GO contents. Tribological test results show that the wear rate of UHMWPE is significantly reduced when GO nanosheets are added up to 1 wt%. Friction in sliding contact of GO-containing nanocomposites is close to pure UHMWPE. The addition of a small amount of GO could obviously increase the micro-hardness of UHMWPE and the

GO/UHMWPE composite, with 0.5 wt% GO having an optimum tensile strength [105]. GO is able to enhance the wear resistance of UHMWPE for the TJRs.

Hydroxyapatite (HA) is a bioactive calcium phosphate ceramic ($Ca_{10}(PO_4)_6(OH)_2$) with chemical and crystallographic characteristics similar to those of natural apatite in bones, and it has been currently used as bioactive coatings on Ti-based alloys for orthopedic applications to improve the integration between the implants and bone tissues. However, the inferior wear resistance of pure HA cannot match the mechanical behavior of natural bone, due to its lower strength and stiffness [147]. To solve this problem, Li [88] attempted to enhance the wear resistance of pure HA by preparing a homogeneous GO/HA composite coating on commercial pure Ti. The results show that compared with pure HA coatings, the GO/HA coatings have enhanced adhesion strength and wear resistance, paving the way for the fabrication of novel graphene-based HA composite coatings for biological applications. Liu [145] found that the antiwear performance of HA improves by the introduction of chemically-modified graphene.

8. Conclusions and Prospect

The preparation of GO is at a mature technology level, partially due to the rapid growth of interest in GO and its derivatives, since graphene was first successfully obtained in 2004. As a result of abundant oxygen-containing functional groups in the GO sheets, GO can be easily modified using chemical and physical methods to produce diverse derivatives for applications. Due to their unique characteristics and compatibility, GO and GOBMs have been under research in the biomedical field [148–150]. GO and its derivatives exhibit promising tribological properties as solid lubricants, oil-based lubricant additives, water-based lubricant additives and fillers for polymer-based composite materials. GOBMs are expected to be promising materials for enhancing the tribological properties of total joint replacements in the physiological environment, as well. Although the applications of GO and its derivatives for bio-tribological systems are less widely reported, the recent advances of GOBMs for bio-tribological applications are significant, which open up exciting opportunities for the broad use of GOBMs in real clinical conditions in the future. In addition, although graphene oxide materials show promise for applications in different biomedical fields, the development of these materials is at a very early stage.

Acknowledgments

Conflicts of Interest

The authors declare no conflict of interest.

References

1. Novoselov, K.S.; Geim, A.K.; Morozov, S.V.; Jiang, D.; Zhang, Y.; Dubonos, S.V.; Grigorieva, I.V.; Firsov, A.A. Electric field effect in atomically thin carbon films. *Science* **2004**, *306*, 666–669.
2. Geim, A.K.; Novoselov, K.S. The rise of graphene. *Nat. Mater.* **2007**, *6*, 183–190.
3. Park, S.J.; Ruoff, R.S. Chemical methods for the production of graphene. *Nat. Nanotechnol.* **2009**, *4*, 217–224.
4. Geim, A.K. Graphene: Status and prospects. *Science* **2009**, *324*, 1530–1534.
5. Avouris, P. Graphene: Electronic and photonic properties and devices. *Nano Lett* **2010**, *10*, 4285–4294.
6. Schwierz, F. Graphene transistors. *Nat. Nanotechnol.* **2010**, *5*, 487–496.
7. Pinto, A.M.; Gonçalves, I.C.; Magalhães, F.D. Graphene-based materials biocompatibility: A review. *Colloids Surf. B: Biointerfaces* **2013**, *111*, 188–202.
8. Wissler, M. Graphite and carbon powders for electrochemical application. *J. Power Sources* **2006**, *156*, 142–150.
9. Szabo´, T.; Szeri, A.; De´ka´ny, I. Composite graphitic nanolayers prepared by self-assembly between finely dispersed graphite oxide and a cationic polymer. *Carbon* **2005**, *43*, 87–94.
10. He, H.; Klinowski, J.; Forster, M.; Lerf, A. A new structure model for graphite oxide. *Chem. Phys. Lett.* **1998**, *287*, 53–56.
11. Lerf, A.; He, H.; Forster,M.; Klinowski, J. Structure of graphite oxide revisited. *J. Phys. Chem. B* **1998**, *102*, 4477–4482.
12. Brodie, B.C. On the atomic weight of graphite. *Philos. Trans. R. Soc. Lond.* **1859**, *149*, 249–259.
13. Young, R.J.; Kinloch, I.A.; Gong, L.; Novoselov, K.S. The mechanics of graphene nanocomposites: A review. *Compos. Sci. Technol.* **2012**, *72*, 1459–1476.
14. Staudenmaier, L. Verfahren zur darstellung der graphitsäure. *Ber. Dtsch. Chem. Ges.* **1898**, *31*, 1481–1487.
15. Ülrich, H.; Rudolf, H. The acid nature and methylation of graphitic oxide. *Ber. Dtsch. Chem. Ges.* **1939**, *72*, 754–771.
16. Ruess, G. Uber das Graphitoxyhydroxyd (Graphitoxyd). *Monatsch. Chem.* **1946**, *76*, 381–417.
17. Hummers, W.S.; Offeman, R.E. Preparation of graphitic oxide. *J. Am. Chem. Soc.* **1958**, *80*, 1339.
18. Dreyer, D.R.; Park, S.J.; Bielawski, C.W.; Ruoff, R.S. The chemistry of graphene oxide. *Chem. Soc. Rev.* **2010**, *39*, 228–240.
19. Zhu, Y.; Mural, S.; Cai, W.; Li, X.; Suk, J.W.; Potts, J.R.; Ruoff, R.S. Graphene and graphene oxide: Synthesis, properties, and applications. *Adv. Mater.* **2010**, *22*, 3906–3924.
20. Kovtyukhova, N.I.; Ollivier, P.J.; Martin, B.R.; Mallouk, T.E.; Chizhik, S.A.; Buzaneva, E.V.; Gorchinskiy, A.D. Layer-by-Layer assembly of ultrathin composite films from micron-sized graphite oxide sheets and polycations. *Chem. Mater.* **1999**, *11*, 771–778.
21. Ma, C.; Liu, W.; Shi, M.; Lang, X.; Chu, Y.; Chen, Z.; Zhao, D.; Lin, W.; Hardacre, C. Low loading platinum nanoparticles on reduced graphene oxide-supported tungsten carbide crystallites as a highly active electrocatalyst for methanol oxidation. *Electrochim. Acta* **2013**, *114*, 133–141.

22. Nikolakopoulou, A.; Tasis, D.; Sygellou, L.; Dracopoulos, V.; Galiotis, C.; Lianos, P. Study of the thermal reduction of graphene oxide and of its application as electrocatalyst in quasi-solid state dye-sensitized solar cells in combination with PEDOT. *Electrochim. Acta* **2013**, *111*, 698–706.

23. Yu, Y; Kang, B.; Lee, Y.; Lee, S.; Ju, B. Effect of fluorine plasma treatment with chemically reduced graphene oxide thin films as hole transport layer in organic solar cells. *Appl. Surf. Sci.* **2013**, *287*, 91–96.

24. Marcano, D.C.; Kosynkin, D.V.; Berlin, J.M.; Sinitskii, A.; Sun, Z.; Slesarev, A.; Alemany, L.B.; Lu, W.; Tour, J.M. Improved synthesis of graphene oxide. *ACS Nano* **2010**, *4*, 4806–4814.

25. Higginbotham, A.L.; Kosynkin, D.V.; Sinitskii, A.; Sun, Z.; Tour, J.M. Lower-defect graphene oxide nanoribbons from multiwalled carbon nanotubes. *ACS Nano* **2010**, *4*, 2059–2069.

26. Li, W.; Xu, Z.; Chen, L.; Shan, M.; Tian, X.; Yang, C.; Lv, H.; Qian, X. A facile method to produce graphene oxide-g-poly (L-lactic acid) as a promising reinforcement for PLLA nanocomposites. *Chem. Eng. J.* **2014**, *237*, 291–299.

27. Mermoux, M.; Chabre, Y.; Rousseau, A. FTIR and ^{13}C NMR study of graphite oxide. *Carbon* **1991**, *29*, 469–474.

28. Ramesh, P.; Bhagyalakshmi, S.; Sampath, S. Preparation and physicochemical and electrochemical characterization of exfoliated graphite oxide. *J. Colloid Interface Sci.* **2004**, *274*, 95–102.

29. McAllister, M.J.; Li, J.; Adamson, D.H.; Schniepp, H.C.; Abdala, A.A.; Liu, J.; Alonso, M.H.; Milius, D.L.; Car, R.; Prud'homme, R.K.; Aksay. I.A. Single sheet functionalized graphene by oxidation and thermal expansion of graphite. *Chem. Mater.* **2007**, *19*, 4396–4404.

30. Compton, O.C.; Nguyen, S.T. Graphene oxide, highly reduced graphene oxide, and graphene: Versatile building blocks for carbon-based materials. *Small* **2010**, *6*, 711–723.

31. Li, P.; Xu, Y.; Cheng, X. Chemisorption of thermal reduced graphene oxide nano-layer film on TNTZ surface and its tribological behavior. *Surf. Coat. Technol.* **2013**, *232*, 331–339.

32. Ou, J.; Wang, J.; Liu, S.; Mu, B.; Ren, J.; Wang, H.; Yang, S. Tribology study of reduced graphene oxide sheets on silicon substrate synthesized via covalent assembly. *Langmuir* **2010**, *26*, 15830–15836.

33. Yang, D.X.; Velamakanni, A.; Bozoklu, G.; Park, S.J.; Stoller, M.; Piner, R.D.; Stankovich, S.; Jung, I.; Field, D.A.; Ventrice, C.A.J.; Ruoff, R.S. Chemical analysis of graphene oxide films after heat and chemical treatments by X-ray photoelectron and Micro-Raman spectroscopy. *Carbon* **2009**, *47*, 145–152.

34. Stankovich, S.; Dikin, D.A.; Piner, R.D.; Kohlhaas, K.A.; Kleinhammes, A.; Jia, Y.; Wu, Y.; Nguyen, S.T.; Ruoff, R.S. Synthesis of graphene-based nanosheets via chemical reduction of exfoliated graphite oxide. *Carbon* **2007**, *45*, 1558–1565.

35. Kozlowski, C.; Sherwood, P.M.A. X-ray photoelectron spectroscopic studies of carbon-fibresurfaces. *J. Chem. Soc. Faraday Trans. I* **1984**, *80*, 2099–2107.

36. Ferrari, A.C.; Meyer, J.C.; Scardaci, V.; Casiraghi, C.; Lazzeri, M.; Mauri, F.; Piscanec, S.; Jiang, D.; Novoselov, K.S.; Roth, S.; *et al.* Raman spectrum of graphene and graphene layers. *Phys. Rev. Lett.* **2006**, *97*, doi:10.1103/PhysRevLett.97.187401.

37. Rourke,J.P.; Pandey, P.A.; Moore, J.J.; Bates, M.; Kinloch, I.A.; Young, R.J.; Wilson, N.R. The real graphene oxide revealed: Stripping the oxidative debris from the graphene-like sheets. *Angew. Chem. Int. Ed.* **2011**, *50*, 3173–3177.

38. Kudin, K.N.; Ozbas, B.; Schniepp, H.C.; Prud'homme, R.K.; Aksay, I.A.; Car, R. Raman spectra of graphite oxide and functionalized graphene sheets. *Nano Lett.* **2008**, *8*, 36–41.

39. Wilson, N.R.; Pandey, P.A.; Beanland, R.; Young, R.J.; Kinloch, I.A.; Gong, L.; Liu, Z.; Suenaga, K.; Rourke, J.P.; York, S.J.; *et al.* Graphene oxide: Structural analysis and application as a highly transparent support for electron microscopy. *ACS Nano* **2009**, *3*, 2547–2556.

40. Kang, H.; Kulkarni, A.; Stankovich, S.; Ruoff, R.S.; Baik, S. Restoring electrical conductivity of dielectrophoretically assembled graphite oxide sheets by thermal and chemical reduction techniques. *Carbon* **2009**, *47*, 1520–1525.

41. Erickson, K.; Erni, R.; Lee, Z.; Alem, N.; Gannett, W.; Zettl, A. Determination of the local chemical structure of graphene oxide and reduced graphene oxide. *Adv. Mater.* **2010**, *22*, 4467–4472.

42. Pacile′, D.; Meyer, J.C.; Rodrı′guez, A.F.; Papagno, M.; Go′mez-Navarro, C.; Sundaram, R.S.; Burghard, M.; Kern, K.; Carbone, C.; Kaiser, U. Electronic properties and atomic structure of graphene oxide membranes. *Carbon* **2011**, *49*, 966–972.

43. Li, D.; MÜller, M.B.; Gilje, S.; Kaner, R.B.; Wallace, G.G. Processable aqueous dispersions of graphene nanosheets. *Nat. Nanotechnol.* **2008**, *3*, 101–105.

44. Paci, J.T.; Belytschko, T.; Schatz, G.C. Computational studies of the structure, behavior upon heating, and mechanical properties of graphite oxide. *J. Phys. Chem. C* **2007**, *111*, 18099–18111.

45. Stankovich, S.; Dikin, D.A.; Dommett, G.H.B.; Kohlhaas, K.M.; Zimney, E.J.; Stach, E.A.; Piner, R.D.; Nguyen, S.T.; Ruoff, R.S. Graphene-based composite materials. *Nature* **2006**, *442*, 282–286.

46. López, V.; Sundaram, R.S.; Gómez-Navarro, C.; Olea, D.; Burghard, M.; Gómez-Herrero, J.; Zamora, F.; Kern, K. Chemical vapor deposition repair of graphene oxide: A route to highly conductive graphene monolayers. *Adv. Mater.* **2009**, *21*, 4683–4686.

47. Zhang, H.; Wang, J.; Yan, Q.; Zheng, W.; Chen, C.; Yu, Z. Vacuum-assisted synthesis of graphene from thermal exfoliation and reduction of graphite oxide. *J. Mater. Chem.* **2011**, *21*, 5392–5397.

48. Gao, W.; Alemany, L.B.; Ci, L.; Ajayan, P.M. New insights into the structure and reduction ofgraphite oxide. *Nat. Chem.* **2009**, *1*, 403–408.

49. Wang, L.; Ye, Y.; Lu, X.; Wu, Y.; Sun, L.; Tan, H.; Xu, F.; Song, Y. Prussian blue nanocubes on nitrobenzene-functionalized reduced graphene oxide and its application for H_2O_2 biosensing. *Electrochim. Acta* **2013**, *114*, 223–232.

50. Wang, G.; Yang, J.; Park, J.; Gou, X.; Wang, B.; Liu, H.; Yao, J. Facile synthesis and characterization of graphene nanosheets. *J. Phys. Chem. C* **2008**, *112*, 8192–8195.

51. Si, Y.; Samulski, E.T. Synthesis of water soluble graphene. *Nano Lett.* **2008**, *8*, 1679–1682.

52. Muszynski, R.; Seger, B.; Kamat, P.V. Decorating graphene sheets with gold nanoparticles. *J. Phys. Chem. C* **2008**, *112*, 5263–5266.

53. Schniepp, H.C.; Li, J.; McAllister, M.J.; Sai, H.; Herrera-Alonso, M.; Adamson, D.H.; Prud'homme, R.K.; Car, R.; Saville, D.A.; Aksay, I.A. Functionalized single graphene sheets derived from splitting graphite oxide. *J. Phys. Chem. B* **2006**, *110*, 8535–8539.

54. Jang, H.; Yun, J.; Kim, D.Y.; Park, D.W.; Na, S.I.; Kim, S.S. Moderately reduced graphene oxide as transparent counter electrodes for dye-sensitized solar cells. *Electrochim. Acta* **2012**, *81*, 301–307.

55. Williams, G.; Serger, B.; Kamat, P.V. TiO_2-graphene nanocomposites: UV-assisted photocatalytic reduction of graphene oxide. *ACS Nano* **2008**, *2*, 1487–1491.

56. Liu, X.; Pan, L.; Zhao, Q.; Lv, T.; Zhu, G.; Chen, T.; Lu, T.; Sun, Z.; Sun, C. UV-assisted photocatalytic synthesis of ZnO-reduced graphene oxide composites with enhanced photocatalytic activity in reduction of Cr(VI). *Chem. Eng. J.* **2012**, *183*, 238–243.

57. Choobtashani, M.; Akhavan, O. Visible light-induced photocatalytic reduction of graphene oxide by tungsten oxide thin films. *Appl. Surf. Sci.* **2013**, *276*, 628–634.

58. Xing, Z.; Chu, Q.; Ren, X.; Tian, J.; Asiri, A.M.; Alamry, K.A.; Al-Youbi, A.O.; Sun, X. Biomolecule-assisted synthesis of nickel sulfides/reduced graphene oxide nanocomposites as electrode materials for supercapacitors. *Electrochem. Commun.* **2013**, *32*, 9–13.

59. Sheng, Z.; Song, L.; Zheng, J.; Hu, D.; He, M.; Zheng, M.; Gao, G.; Gong, P.; Zhang, P.; Ma, Y.; Cai, L. Protein-assisted fabrication of nano-reduced graphene oxide for combined *in vivo* photo acoustic imaging and photo thermal therapy. *Biomaterials* **2013**, *34*, 5236–5243.

60. Akhavan, O.; Ghaderi, E.; Abouei, E.; Hatamie, S.; Ghasemi, E. Accelerated differentiation of neural stem cells in toneurons on ginseng-reduced graphene oxide sheets. *Carbon* **2014**, *66*, 395–406.

61. Kong, C.; Song, W.; Meziani, M.J.; Tackett, K.N.; Cao, L.; Farr, A.J.; Anderson, A.; Sun, Y. Supercritical fluid conversion of graphene oxides. *J. Supercrit. Fluids* **2012**, *61*, 206–211.

62. Zhou, M.; Wang, Y.; Zhai, Y.; Zhai, J.; Ren, W.; Wang, F.; Dong, S. Controlled synthesis of large-area and patterned electrochemically reduced graphene oxide films. *Chem. A Eur. J.* **2009**, *15*, 6116–6120.

63. Sutar, D.S.; Narayanam, P.K.; Singh, G.; Botcha, V.D.; Talwar, S.S.; Srinivasa, R.S.; Major, S.S. Spectroscopic studies of large sheets of graphene oxide and reduced graphene oxide monolayers prepared by Langmuir-Blodgett technique. *Thin Solid Film* **2012**, *520*, 5991–5996.

64. Bourlinos, A.B.; Gournis, D.; Petridis, D.; Szabo, T.; Szeri, A.; Dekany, I. Graphite oxide: Chemical reduction to graphite and surface modification with primary aliphatic amines and amino acids. *Langmuir* **2003**, *19*, 6050–6055.

65. Matsuo, Y.; Miyabe, T.; Fukutsuka, T.; Sugie, Y. Preparation and characterization of alkylamine-intercalated graphite oxides. *Carbon* **2007**, *45*, 1005–1012.

66. Wang, S.; Chia, P.J.; Chua, L.L.; Zhao, L.H.; Png, R.Q.; Sivaramakrishnan, S.; Zhou, M.; Goh, R.G.S.; Friend, R.H.; Wee, A.T.S.; Ho, P.K.H. Band-like transport in surface-functionalized highly solution-processable graphene nanosheets. *Adv. Mater.* **2008**, *20*, 3440–3446.

67. Shan, C.; Yang, H.; Han, D.; Zhang, Q.; Ivaska, A.; Niu, L. Water-soluble graphene covalently functionalized by biocompatible poly-L-lysine. *Langmuir* **2009**, *25*, 12030–12033.

68. Wang, G.; Shen, X.; Wang, B.; Yao, J.; Park, J. Synthesis and characterization of hydrophilic and organophilic graphene nanosheets. *Carbon* **2009**, *47*, 1359–1364.

69. Shen, J.; Shi, M.; Ma, H.; Yan, B.; Li, N.; Hu, Y.; Ye, M. Synthesis of hydrophilic and organophilic chemically modified graphene oxide sheets. *J. Colloid Interface Sci.* **2010**, *351*, 366–370.

70. Yuan, B.; Bao, C.; Song, L.; Hong, N.; Liew, K.M.; Hu, Y. Preparation of functionalized graphene oxide/polypropylene nanocomposite with significantly improved thermal stability and studies on the crystallization behavior and mechanical properties. *Chem. Eng. J.* **2014**, *237*, 411–420.

71. Xu, L.; Yang, W.; Neoh, K.G.; Kang, E.; Fu, G. Dopamine-induced reduction and functionalization of graphene oxide nanosheets. *Macromolecules* **2010**, *43*, 8336–8339.

72. Yang, H.; Shan, C.; Li, F.; Han, D.; Zhang, Q.; Niu, L. Covalent functionalization of poly disperse chemically-converted graphene sheets with amine-terminated ionic liquid. *Chem. Commun.* **2009**, doi:10.1039/b905085j.

73. Yan, J.; Chen, G.; Cao, J.; Yang, W.; Xie, B.; Yang, M. Functionalized graphene oxide with ethylenediamine and 1,6-hexanediamine. *New Carbon Mater.* **2012**, *27*, 370–376.

74. Liu, Z.; Xu, Y.; Zhang,X .; Zhang, X.; Chen, Y.; Tian, J. Porphyrin and fullerene covalently functionalized graphene hybrid materials with large nonlinear optical properties. *J. Phys. Chem. B* **2009**, *113*, 9681–9686.

75. Liu, Z.; Robinson, J.T.; Sun, X.; Dai, H. PEGylated nano graphene oxide for delivery of water-insoluble cancer drugs. *J. Am. Chem. Soc.* **2008**, *130*, 10876–10877.

76. Veca, L.M.; Lu, F.; Meziani, M.J.; Cao, L.; Zhang, P.; Qi, G.; Qu, L.; Shrestha, M.; Sun, Y.P. Polymer functionalization and solubilization of carbon nanosheets. *Chem. Commun.* **2009**, doi:10.1039/b900590k.

77. Tang, X.; Li, W.; Yu, Z.; Rafiee, M.A.; Rafiee, J.; Yavari, F.; Koratkar, N. Enhanced thermal stability in graphene oxide covalently functionalized with 2-amino-4,6-didodecylamino-1,3,5-triazine. *Carbon* **2011**, *49*, 1258–1265.

78. Lu, W.; Ning, R.; Qin, X.; Zhang, Y.; Chang, G.; Liu, S.; Luo, Y.; Sun, X. Synthesis of Au nanoparticles decorated graphene oxide nanosheets: Noncovalent functionalization by TWEEN 20 *in situ* reduction of aqueous chloroaurate ions for hydrazine detection and catalytic reduction of 4-nitrophenol. *J. Hazard. Mater.* **2011**, *197*, 320–326.

79. Su, S.; Chen, B.; He, M.; Hu, B.; Xiao, Z. Determination of trace/ultratrace rare earth elements in environmental samples by ICP-MS after magnetic solid phase extraction with Fe3O4@SiO2@polyaniline–graphene oxide composite. *Talanta* **2014**, *119*, 458–466.

80. Choi, E.; Han, T.; Hong, J.; Kim, J.E.; Lee, S.H.; Kim, H.W.; Kim, S.O. Noncovalent functionalization of graphene with end-functional polymers. *J. Mater. Chem.* **2010**, *20*, 1907–1912.

81. Pan, Y.; Bao, H.; Sahoo, N.G.; Wu, T.; Li, L. Water-soluble poly(N-isopropylacrylamide)-graphene sheets synthesized via click chemistry for drug delivery. *Adv. Funct. Mater.* **2011**, *21*, 2754–2763.

82. Geng, J.; Jung, H. Porphyrin functionalized graphene sheets in aqueous suspensions: From the preparation of graphene sheets to highly conductive graphene films. *J. Phys. Chem. C* **2010**, *114*, 8227–8234.

83. Ghosh, A.; Rao, K.V.; George, S.J.; Rao, C.N.R. Noncovalent functionalization, exfoliation, and solubilization of graphene in water by employing a fluorescent coronene carboxylate. *Chem. Eur. J.* **2010**, *16*, 2700–2704.

84. Yang, Q.; Pan, X.; Huang, F.; Li, K. Fabrication of high-concentration and stable aqueous suspensions of graphene nanosheets by noncovalent functionalization with lignin and cellulose derivatives. *J. Phys. Chem. C* **2010**, *114*, 3811–3816.

85. Liu, Q.; Shi, J.; Sun, J.; Wang, T.; Zeng, L.; Jiang, G. Graphene and graphene oxide sheets supported on silica as versatile and high-performance adsorbents for solid-phase extraction. *Angew. Chem. Int. Ed.* **2011**, *50*, 5913–5917.

86. Eda, G.; Chhowalla, M. Chemically derived graphene oxide: Towards large-area thin-film electronics and optoelectronics. *Adv. Mater.* **2010**, *22*, 2392–2415.

87. Li, M.; Liu, Q.; Jia, Z.; Xu, X.; Shi, Y.; Cheng, Y.; Zheng, Y.; Xi, T.; Wei, S. Electrophoretic deposition and electrochemical behavior of novel graphene oxide-hyaluronic acid-hydroxyapatite nanocomposite coatings. *Appl. Surf. Sci.* **2013**, *284*, 804–810.

88. Li, M.; Liu, Q.; Jia, Z.; Xu, X.; Cheng, Y.; Zheng, Y.; Xi, T.; Wei, S. Graphene oxide/hydroxyapatite composite coatings fabricated by electrophoretic nanotechnology for biological applications. *Carbon* **2014**, *67*, 185–197.

89. Khoa, N.T.; Pyun, M.W.; Yoo, D.H.; Kim, S.W.; Leem, J.Y.; Kim, E.J.; Hahn, S.H. Photodecomposition effects of graphene oxide coated on TiO_2 thin film prepared by electron-beam evaporation method. *Thin Solid Films* **2012**, *520*, 5417–5420.

90. Min, Y.; Zhang, K.; Zhao, W.; Zheng, F.; Chen, Y.; Zhang, Y. Enhanced chemical interaction between TiO_2 and graphene oxide for photocatalytic decolorization of methylene blue. *Chem. Eng. J.* **2012**, *193–194*, 203–210.

91. Akhavan, O.; Ghaderi, E. Photocatalyticr eduction of graphene oxide nanosheets on TiO_2 thin film for photo inactivation of bacteria in solar light irradiation. *J. Phys. Chem. C* **2009**, *113*, 20214–20220.

92. Zhang, S.; Du, Z.; Li, G. Graphene-supported zinc oxide solid-phase micro extraction coating with enhanced selectivity and sensitivity for the determination of sulfur volatiles in Allium species. *J. Chromatogr. A* **2012**, *1260*, 1–8.

93. Yao, Y.; Chen, X.; Guo, H.; Wu, Z. Graphene oxide thin film coated quartz crystal microbalance for humidity detection. *Appl. Surf. Sci.* **2011**, *257*, 7778–7782.

94. Watcharotone, S.; Dikin, D.A.; Stankovich, S.; Piner, R.; Jung, I.; Dommett, G.H.B.; Evmenenko, G.; Wu, S.; Chen, S.; Liu, C.; *et al.* Graphene-silica composite thin films as transparent conductors. *Nano Lett.* **2007**, *7*, 1888–1892.

95. Cote, L.J.; Kim, F.; Huang, J. Langmuir-Blodgett assembly of graphite oxide single layers. *J. Am. Chem. Soc.* **2009**, *131*, 1043–1049.

96. Valentini, L.; Bon, S.B.; Monticelli, O.; Kenny, J.M. Deposition of amino-functionalized polyhedral oligomericsilsesquioxanes on graphene oxide sheets immobilized onto an amino-silane modified silicon surface. *J. Mater. Chem.* **2012**, *22*, 6213–6217.

97. Liang, H.; Bu, Y.; Zhang, J.; Cao, Z.; Liang, A. Graphene oxide film as solid lubricants. *ACS Appl. Mater. Interfaces* **2013**, *5*, 6369–6375.

98. Fan, H.; Yao, F.; Xu, S.; Chen, G. Microchip bioreactors based on trypsin-immobilized graphene oxide-poly (urea-formaldehyde) composite coating for efficient peptide mapping. *Talanta* **2013**, *117*, 119–126.

99. Singh, B.P.; Nayak, S.; Nanda, K.K.; Jena, B.K.; Bhattacharjee, S.; Besra, L. The production of a corrosion resistant graphene reinforced composite coating on copper by electrophoretic deposition. *Carbon* **2013**, *61*, 47–56.

100. Singh, B.P.; Jena, B.K.; Bhattacharjee, S.; Besra, L. Development of oxidation and corrosion resistance hydrophobic graphene oxide-polymer composite coating on copper. *Surf. Coat. Technol.* **2013**, *232*, 475–481.

101. Sahu, S.C.; Samantara, A.K.; Seth, M.; Parwaiz, S.; Singh, B.P.; Rath, P.C.; Jena, B.K. A facile electrochemical approach for development of highly corrosion protective coatings using graphene nanosheets. *Electrochem. Commun.* **2013**, *32*, 22–26.

102. Zhu, Y.; Yu, L.; Wang, X.; Zhou, Y.; Ye, H. A novel monolithic Pd catalyst supported on cordierite with graphene coating. *Catal. Commun.* **2013**, *40*, 98–102.

103. Domingues, S.H.; Kholmanov, I.N.; Kim, T.Y.; Kim,J.Y.; Tan, C.; Chou, H.; Alieva, Z.A.; Piner, R.; Zarbin, A.J. G.; Ruoff, R.S. Reduction of graphene oxide films on Al foil for hybrid transparent conductive film applications. *Carbon* **2013**, *63*, 454–459.

104. Moniruzzaman, M.; Winey, K. Polymer nanocomposites containing carbon nanotubes. *Macromolecules* **2006**, *39*, 5194–5205.

105. Chen, Y.; Qi, Y.; Tai, Z.; Yan, X.; Zhu, F.; Xue, Q. Preparation, mechanical properties and biocompatibility of graphene oxide/ultrahigh molecular weight polyethylene composites. *Eur. Polym. J.* **2012**, *48*, 1026–1033.

106. Tai. Z.; Chen, Y.; An, Y.; Yan, X.; Xue, Q. Tribological behavior of UHMWPE reinforced with graphene oxide nanosheets. *Tribollett* **2012**, *46*, 55–63.

107. Suñer, S; Emami, N. Investigation of graphene oxide as reinforcement for orthopaedic applications. *Tribology* **2014**, *8*, 1–6.

108. Fim, F.C.; Guterres, J.M.; Basso, N.R.S.; Galland, G.B. Polyethylene/graphite nanocomposites obtained by *in situ* polymerization. *J. Polym. Sci. Part A: Polym. Chem.* **2010**, *48*, 692–698.

109. Huang, Y.; Qin, Y.; Zhou, Y.; Niu, H.; Yu, Z.; Dong, J. Polypropylene/graphene oxide nanocomposites prepared by *in situ* Ziegler–Natta polymerization. *Chem. Mater.* **2010**, *22*, 4096–4102.

110. Potts, J.R.; Lee, S.H.; Alam, T.M.; An, J.H.; Stoller, M.D. Piner, R.D.; Ruoff, R.S. Thermomechanical properties of chemically modified graphene/poly(methyl methacrylate) composites made by *in situ* polymerization. *Carbon* **2011**, *49*, 2615–2623.

111. Wang, J.; Xu, Y.; Zhu, J.; Ren, P. Electrochemical *in situ* polymerization of reduced graphene oxide/polypyrrole composite with high power density. *J. Power Sources* **2012**, *208*, 138–143.

112. Wang, X.; Yang, C.; Li, H.D.; Liu, P. Synthesis and electrochemical performance of well-defined flake-shaped sulfonated graphene/polypyrrole composites via facile *in situ* doping polymerization. *Electrochim. Acta* **2013**, *111*, 729–737.

113. Lin, Y.; Hsu, F.; Wu, T. Enhanced conductivity and thermal stability of conductive polyaniline/graphene composite synthesized by *in situ* chemical oxidation polymerization with sodium dodecyl sulfate. *Synth. Met.* **2013**, *184*, 29–34.

114. Qian, X.; Song, L.; Yu, B.; Yang, W.; Wang, B.; Hu, Y.; Yuen, R.K.K. One-pot surface functionalization and reduction of graphene oxide with long-chain molecules: Preparation and its enhancement on the thermal and mechanical properties of polyurea. *Chem. Eng. J.* **2014**, *236*, 233–241.

115. Paszkiewicz, S.; Szymczyk, A.; Špitalsky´, Z.; Mosnacek, J.; Kwiatkowski, K.; Rosłanie, Z. Structure and properties of nanocomposites based on PTT-block-PTMO copolymer and graphene oxide prepared by *in situ* polymerization. *Eur. Polym. J.* **2014**, *50*, 69–77.

116. Ruiz, O.N.; Fernando, K.A.S.; Wang, B.; Brown, N.A.; Luo, P.; McNamara, N.D.; Vangsness, M.; Sun, Y.; Bunker, C.E. Graphene oxide: A nonspecific enhancer of cellular growth. *ACS Nano* **2011**, *5*, 8100–8107.

117. Liu, Y.; Yu, D.; Zeng, C.; Miao, Z.; Dai, L. Biocompatible graphene oxide-based glucose biosensors. *Langmuir* **2010**, *26*, 6158–6160.

118. Sasidharan, A.; Panchakarla, L.S.; Chandran, P.; Menon, D.; Nair, S.; Raob, C.N.R.; Koyakutty, M. Differential nano-bio interactions and toxicity effects of pristine *versus* functionalized graphene. *Nanoscale* **2011**, *3*, 2461–2466.

119. Dong, H.; Ding, L.; Yan, F.; Ji, H.; Ju, H. The use of poly ethylenimine-grafted graphene nanoribbon for cellular delivery of locked nucleic acid modified molecular beacon for recognition of microRNA. *Biomaterials* **2011**, *32*, 3875–3882.

120. Hu, W.; Peng, C.; Lv, M.; Li, X.; Zhang, Y.; Chen, N.; Fan, C.; Huang, Q. Protein corona-mediated mitigation of cytotoxicity of graphene oxide. *ACS Nano* **2011**, *5*, 3693–3700.

121. Pinto, A.M.; Moreira, S.M.; Gama, F.M.; Gonçalves, I.C.; Magalhães, F.D. Biocompatibility of poly (lactic acid) with incorporated graphene-based materials. *Colloids Surf. B: Biointerfaces* **2013**, *104*, 229–238.

122. Ma, H.; Su, W.; Tai, Z.; Sun, D.; Yan, X.; Liu, B.; Xue, Q. Preparation and cytocompatibility of polylactic acid/hydroxyapatite/graphene oxide nanocomposite fibrous membrane. *Chin. Sci. Bull.* **2012**, *57*, 3051–3058.

123. Yan, X.; Chen, J.; Yang, J.; Xue, Q.; Miele, P. Fabrication of free-standing, electrochemically active, and biocompatible graphene oxide-polyaniline and graphene-polyanilinehybrid papers. *ACS Appl. Mater. Interfaces* **2010**, *2*, 2521–2529.

124. Gurunathan, S.; Han, J.W.; Eppakayala, V.; Kim, J.H. Biocompatibility of microbially reduced graphene oxide in primary mouseembryonic fibroblast cells. *Colloids Surf. B: Biointerfaces* **2013**, *105*, 58–66.

125. Chen, H.; Muller, M.B.; Gilmore, K.J.; Wallace, G.G.; Li, D. Mechanically Strong, Electrically Conductive, and Biocompatible Graphene Paper. *Adv. Mater.* **2008**, *20*, 3557–3561.

126. Agarwal, S.; Zhou, X.; Ye, F.; He, Q.; Chen, G.C.; Soo, J.; Boey, F.; Zhang, H.; Chen, P. Interfacing Live Cells with Nanocarbon Substrates. *Langmuir* **2010**, *26*, 2244–2247.

127. Park, S.; Mohanty, N.; Suk, J.W.; Nagaraja, A.; An, J.; Piner, R.D.; Cai, W.; Dreyer, D.R.; Berry, V.; Ruoff, R.S. Biocompatible, Robust Free-Standing Paper Composed of a TWEEN/Graphene Composite. *Adv. Mater.* **2010**, *22*, 1736–1740.

128. Liao, K.H.; Lin, Y.S.; Macosko, C.W.; Haynes, C.L. Cytotoxicity of Graphene Oxide and Graphene in Human Erythrocytes and Skin Fibroblasts. *ACS Appl. Mater. Interfaces* **2011**, *3*, 2607–2615.

129. Liu, Y.; Zhang, Y.; Zhang, T.; Jiang, Y.; Liu, X. Synthesis, characterization and cytotoxicity of phosphorylcholine oligomer grafted grapheme oxide. *Carbon* **2014**, *71*, 166–175.

130. Ou, J.; Wang, Y.; Wang, J.; Liu, S.; Li, Z.; Yang, S. Self-assembly of octadecyltrichlorosilane on graphene oxideand the tribological performances of the resultant film. *J. Phys. Chem. C* **2011**, *115*, 10080–10086.

131. Li, P.; Zhou, H.; Cheng, X. Nano/micro tribological behaviors of a self-assembled graphene oxide nanolayer on Ti/titanium alloy substrates. *Appl. Surface Sci.* **2013**, *285P*, 937–944.

132. Shen, X.; Pei, X.; Fu, S.; Friedrich, K. Significantly modified tribological performance of epoxy nanocomposites at very low graphene oxide content. *Polymer* **2013**, *54*, 1234–1242.

133. Shen, X.; Pei, X.; Liu, Y.; Fu, S. Tribological performance of carbon nanotube-graphene oxide hybrid/epoxy composites. *Compos. Part B* **2014**, *57*,120–125.

134. Li, Y.; Wang, Q.; Wang, T.; Pan, G. Preparation and tribological properties of graphene oxide/nitrile rubber nanocomposites. *J. Mater. Sci.* **2012**, *47*, 730–738.

135. Mo, Y.; Yang, M.; Lu, Z.; Huang, F. Preparation and tribological performance of chemically-modified reduced graphene oxide/polyacrylonitrile composites. *Compos. Part A* **2013**, *54*, 153–158.

136. Thangavel, E.; Ramasundaram, S.; Pitchaimuthu, S.; Hong, S.W.; Lee, S.Y.; Yoo, S.S.; Kim, D.E.; Ito, E.; Kang, Y. Structural and tribological characteristics of poly(vinylidene fluoride)/functionalized graphene oxide nanocomposite thin films. *Compos. Sci. Technol.* **2014**, *90*, 187–192.

137. Kandanur, S.S.; Rafiee, M.A.; Yavari, F.; Schrameyer, M.; Yu, Z.Z.; lanchet, T.A.; Koratkar, N. Suppression of wear in graphene polymer composites. *Carbon* **2012**, *50*, 3178–3183.

138. Zhang, W.; Zhou, M.; Zhu, H.; Tian, Y.; Wang, K.; Wei, J.; Ji, F.; Li, X.; Li, Z.; Zhang, P.; Wu, D. Tribological properties of oleicacid-modified graphene as lubricant oil additives. *J. Phys. D: Appl. Phys.* **2011**, *44*, doi:10.1088/0022-3727/44/20/205303.

139. Eswaraiah, V.; Sankaranarayanan, V.; Ramaprabhu, S. Graphene-based engine oil nanofluids for tribological applications. *ACS Appl. Mater. Interfaces* **2011**, *3*, 4221–4227.

140. Choudhary, S.; Mungse, H.P.; Khatri, O.P. Dispersion of alkylated graphene in organic solvents and its potential for lubrication applications. *J. Mater. Chem.* **2012**, *22*, 21032–21039.

141. Song, H.; Li, N. Frictional behavior of oxide graphene nanosheets as water-base lubricant additive. *Appl. Phys. A: Mater. Sci. Process.* **2011**, *105*, 827–832.

142. Kinoshita, H.; Nishina, Y.; Alias, A.A.; Fujii, M. Tribological properties of monolayer graphene oxide sheets as water-based lubricant additives. *Carbon* **2014**, *66*, 720–723.

143. Hoseini, M.; Jedenmalm, A.; Boldizar, A. Tribological investigation of coatings for artificial joints. *Wear* **2008**, *264*, 958–966.

144. Sonntag, R.; Reinders, J.; Kretzer, J.P. What's next? Alternative materials for articulation in total joint replacement. *Acta Biomater.* **2012**, *8*, 2434–2441.

145. Liu, Y.; Dang, Z.; Wang, Y.; Huang, J.; Li, H. Hydroxyapatite/graphene-nanosheet composite coatings deposited by vacuum cold spraying for biomedical applications: Inherited nanostructures and enhanced properties. *Carbon* **2014**, *67*, 250–259.

146. Pan, Y.; Sahoo, N.G.; Li, L. The application of graphene oxide in drug delivery. *Exp. Opin. Drug Deliv.* **2012**, *12*, 13265–13276.

147. Kurtz, S.M. *The UHMWPE Handbook: Ultra-High Molecular Weight Polyethylene in Total Joint Replacement*; Elsevier Academic Press: Boston, UK, 2004.
148. Fang, L.; Leng, Y.; Gao, P. Processing and mechanical properties of HA/UHMWPE nanocomposites. *Biomaterials* **2006**, *27*, 3701–3707.
149. Bao, H.; Pan, Y.; Li, L. Recent advances in graphene-based nanomaterials for biomedical applications. *Nano Life* **2012**, *2*, 1–15.
150. Wang, Y.; Li, Z.; Wang, J.; Li, J.; Lin, Y. Graphene and graphene oxide: Biofunctionalization and applications in biotechnology. *Trends Biotechnol.* **2011**, *29*, 205–212.